theless, the depleted models experience much smaller increases in radius. This behavior indicates that the overall luminosity of the stars is determined by the contracting core, and has relatively little to do with the composition gradient between the core and the envelope. Larger compositional gradients appear to be a vital element in determining the relative ability of the star to expand.

4.3. *Photospheric Opacity*

In equilibrium, the internal luminosity L_* of the star is radiated into space. The surface properties of the star obey the usual relation

$$L_* = 4\pi R_*^2 \sigma_B T_*^4 , \tag{4.1}$$

where R_* is the stellar radius, T_* is the effective surface temperature, and σ_B is the Stefan-Boltzmann constant. Faced with the increasing luminosity described above, a star in equilibrium must either increase its radius or increase its temperature (or both). Numerically we find that very low mass stars, $M_* \sim 0.1\ M_\odot$, become blue dwarfs, i.e., they increase their temperatures. On the other hand, higher mass stars $M_\odot \sim 0.25\ M_\odot$, tend to increase their radius and keep the temperature roughly constant. The star could also depart from equilibrium; this point is taken up below.

Near the stellar surface, convection must become superadiabatic, and hence increasingly ineffective. Stars have no choice but to radiate from their photospheres. The consequences of this requirement are shown in Figure 6, where we plot the evolution of the $M_* = 0.06, 0.08, 0.10, 0.12, 0.16$, and $0.25\ M_\odot$ models as a function of their photospheric densities and temperatures. The size of a point corresponding to a converged model is in direct proportion to the stellar radius. The expansion of the $M_* = 0.25\ M_\odot$ model as it becomes a red giant is dramatically visible. The hydrogen-rich opacity table has been plotted as a gray-scale backdrop to the diagram; darker regions correspond to larger opacities. The general increase in opacity toward the top of the diagram is due to H^- and hydrogen ionization, whereas the opaque region below $\log_{10} T \approx 3.3$ is due to molecules and grains. This figure demonstrates that in order to achieve efficient radiation, there is a general overall tendency for evolving stars to adjust their envelope structure so as to occupy more transparent regions in the photospheric ρ-T diagram.

If the opacity in the stellar photosphere is a sharply increasing function of temperature, then the requirement that the star is in equilibrium as well as radiating from its photosphere implies an effective upper bound

$$T_* \leq T_{\max} \tag{4.2}$$

for the photosphere. Once the star is in a configuration where the photospheric temperature is approaching $T_{\max}$, the star has no choice but to increase its radius rather than increase its temperature. In this manner the opacity controls, in part, when a star becomes a red giant.

The maximum temperature $T_{\max}$ is determined by the opacity, which, in evolving low-mass stars, is strongly dependent on the relative hydrogen fraction in the atmosphere. Our evolutionary calculations show that as the overall stellar mass increases, radiative cores appear earlier

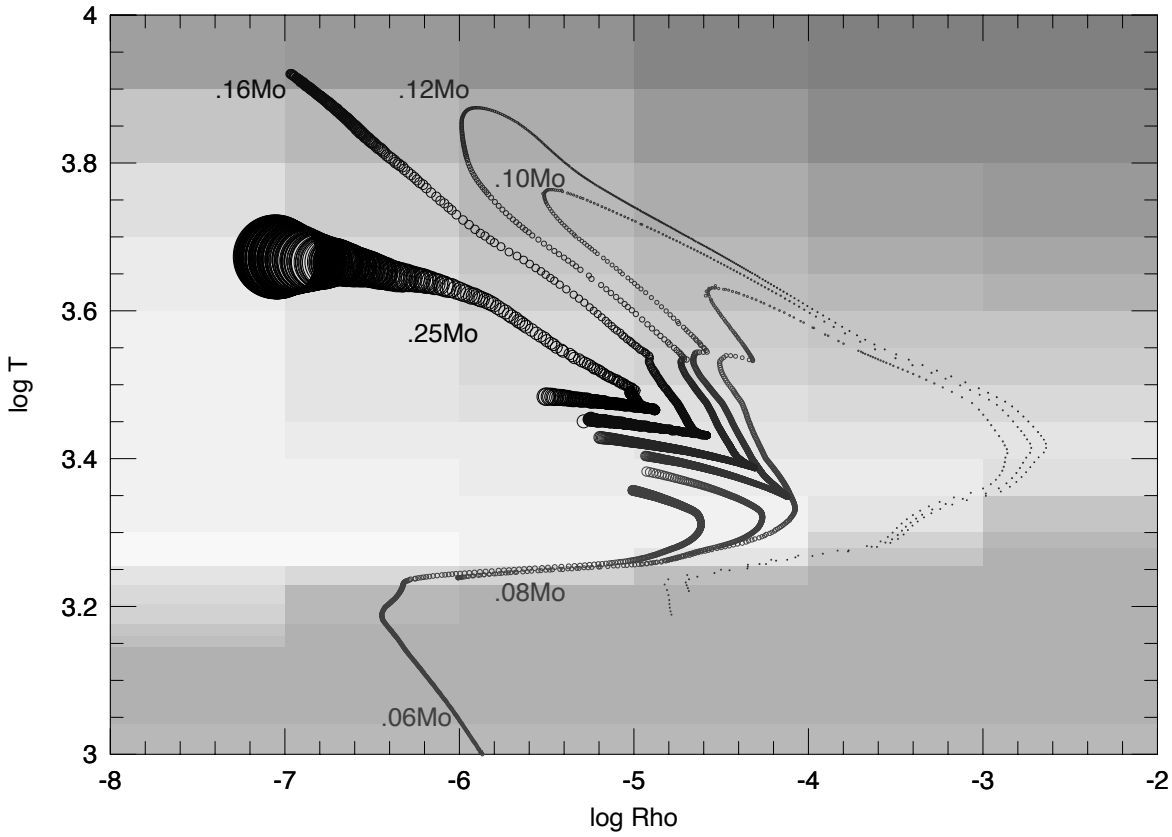

FIG. 6.—Photospheric evolution in the density-temperature plane. The evolutionary sequences are plotted on top of the hydrogen-rich opacity table. Darker shades of gray represent higher opacities. The size of the open circle representing a converged model is in proportion to the actual radius of the star. The stars begin their evolution on the Hayashi track, clustered fairly close together near the point $\log_{10} T \approx 3.3$, $\log_{10} \rho \approx -5.5$. Notice that the $M_* = 0.08$ model slides all the way along the grain opacity boundary to a photospheric density $\log_{10} \rho \approx -5.5$ before reaching the main sequence.